Construction and Building Materials 186 (2018) 31–41

Contents lists available at ScienceDirect

Construction and Building Materials

journal homepage: www.elsevier.com/locate/conbuildmat

Effect of microwave heating damage on the electrical, thermal and mechanical properties of fibre-reinforced cement mortars

R. Borinaga-Treviño [a,*], A. Orbe [a], J. Norambuena-Contreras [b], J. Canales [a]

[a] Department of Mechanical Engineering, University of the Basque Country UPV/EHU, Plaza Ingeniero Torres Quevedo 1, 48013 Bilbao, Spain
[b] LabMAT, Department of Civil and Environmental Engineering, University of Bío-Bío, Concepción, Chile

HIGHLIGHTS

- Microwave heating harm on steel fibre-reinforced and plain mortars was measured.
- Microwave heating reduces flexural strength on non-reinforced mortars.
- Steel fibres reduced mechanical damage on reinforced mortars.
- Thermal and electrical tests did not detect the mechanical damage in any case.

ARTICLE INFO

Article history:
Received 11 April 2018
Received in revised form 12 June 2018
Accepted 13 July 2018

Keywords:
Cement-based mortars
Microwave heating
Thermal conductivity
Electrical resistivity
Mechanical damage
Fibre influence

ABSTRACT

Nowadays, refurbishing of existing structures has gained interest in order to reduce both the construction materials used and the construction and demolition waste production. For that purpose, there are several methods for demolishing the damaged parts, but most of the alternatives involve high noise and dust production, which are in contraposition when structures are in urban areas. Among all the existing methods, this paper studies the possibility of using microwave heating as a demolition method, either by damaging the bulk material or the mortar to concrete interface. With that in mind, the effect of microwave heating time (range 120–600 s) on the physical, thermal, electrical, mechanical and bonding properties of steel fibre-reinforced and non-reinforced cement mortars was analysed. The aim of the paper is to establish possible correlations between the mentioned properties and the damage level caused by microwave heating. Although the results prove that pore pressure increment due to microwave heating can cause the reduction of flexural strength up to the rupture of the specimens, this fact cannot be extended to all the properties or mortar types. The fibre reinforcement plays a key role to restrain the damage. Thermal conductivity and electrical resistivity are obviously different in reinforced and non-reinforced mortars due to the inclusions of the metallic fibres. However, after undergoing microwave heating those properties were not noticeably altered nor follow a trend linked to the heating time. It is assumed that the water migration and evaporation processes are the main cause. Although the flexural strength reduction was gradual for non-reinforced mortars until total failure, the reinforced specimens only showed a 13% of reduction for the first 120 s, remaining almost constant afterwards. Although it was proved that the fibres increase the temperature on the specimen surface and its adhesion to the matrix is altered, their crack bridging effect overcomes further damage.

1. Introduction

In order to reduce the construction and material costs on the construction industry, reuse of old structures for new uses has gained interest. For that purpose, structures have to be restored and/or reinforced. For concrete structures, the existing concrete and reinforcement condition must be evaluated. If any of the materials involved does not fulfil the requirements imposed by the existing EN-1504 standards, they need to be replaced in order to guarantee a minimum quality of the refurbished structure. In any case, concrete must be removed either because of its own damage, or to reach and remove the corroded rebars. For the surface concrete removal, there are numerous alternatives [1–3], such as: (1) by impact: chiselling, hammering, by explosives; (2) by cutting it: drilling, sawing, by shear; (3) by bursting it: by explosives,

* Corresponding author.
E-mail address: roque.borinaga@ehu.eus (R. Borinaga-Treviño).

https://doi.org/10.1016/j.conbuildmat.2018.07.108
0950-0618/

Nomenclature

MW	*microwave*
EN	*European Standard*
R	*non-reinforced reference mortar*
S	*brass covered steel fibre reinforced mortar*
F_b	*maximum load registered during the contact bonding surface test* (N)
σ_b	*contact surface bonding stress* (MPa)
β	*bonded surface to load direction angle* (°)
ρ	*mortar dry apparent density* (kg/m^3)
ρ_w	*water density* (kg/m^3)
N	*mortar water accessible porosity* (–)
m_{sat}	*mortar water-saturated mass* (g)
m_{dry}	*mortar oven-dried mass* (g)
m_{dry}	*mortar mass submerged into water* (g)
λ	*mortar apparent thermal conductivity* (W/(m K))
α	*mortar apparent thermal diffusivity* (mm^2/s)
P_0	*heating rate used to determine thermal conductivity* (W)
a	*radius of the HOTDISK M1 sensor* (mm)
t	*time since the beginning of the thermal conductivity test* (s)
τ	*dimensionless time* (–)
ρ'	*electrical resistivity* (Ωm)
r	*electrical resistance* (Ω)
L	*length of the 40 × 40 × 160* mm^3 *prismatic specimen*
s	*cross section of the 40 × 40 × 160* mm^3 *prismatic specimen*

expansive cement and chemical agents, by hydraulic expanding devices; (4) abrading methods: sand blasting, shot blasting, milling; (5) low to high pressure hydro-demolition methods; and (6) thermal methods: flame lance, laser beam, electron beam, arc heating, high-voltage pulses, microwave heating, induction heating, microwave-drilling.

Usually, refurbishments are to be done in urban areas, where noise and vibrations are a real concern and thus must be minimised. In that case, expansive methods, hydro-demolition and thermal methods have proven to be successful. Nevertheless, most of the expansive methods require drilling, which still causes disturbances and the hydro-demolition requires water, which is a valuable resource that is not always available in the amount required [3].

Among the existing thermal methods, this paper focuses on the use of microwave heating to locally damage concrete. In that way, Ong and Akbarnezhad [3] and Makul et al. [4] summarised the different uses of microwave energy on cement-based materials. Microwaves have been studied as a non-destructive method for evaluating damage on concrete and reinforcing bars [5–10]. Different studies proved that microwaves could be used to improve the early strength of mortars by accelerating its hardening process [11–19], but they decreased the 28 day compressive strength of concretes. However, microwaves have also been used to remove contaminated superficial concrete [3]. Jerby et al. [20] used high intensity microwave heating to locally melt concrete, providing a non-abrading drilling method. Other authors [21–23] have also used microwave energy to eliminate cement paste from the crushed construction and demolition wastes in order to improve the quality of the aggregates enabling their use in new concrete manufacturing.

Once the damaged superficial concrete is removed, old concrete is replaced by specially designed mixes for repairing structures. The main goal is to protect the old and new reinforcement while contributing its compressive strength on the repaired area. Thus, steel fibre-reinforced mortars and concretes are widely used to repair structures and industrial pavements, but also in the concrete precast industry due to their higher toughness and durability [24]. Particularly, fibre-reinforced cementitious materials are used on pavements, tunnel dowels, railway precast slab tracks and so on. Hence, the use of fibre-reinforced composites is increasing, but its demolition could be more problematic precisely due to its higher impact resistance. However, there is scarce literature related to the demolition of fibre-reinforced concretes.

This paper aims to evaluate the effect of damage caused by microwave heating on the electrical, thermal and mechanical properties of fibre-reinforced cement mortars. For that purpose, a commercial floor slab repairing mortar was used with, and without, steel fibre-reinforcement. Thermal, electrical, mechanical and bonding properties of the cement mortar specimens were evaluated for different microwave heating times in order to determine the damage caused by the heating procedure.

2. Materials and methods

This section describes the materials and experimental programme followed in this study. Fig. 1 shows the different test methods used on the cement mortar specimens with, and without, steel fibres.

2.1. Materials and mix proportions

The Mapei Planitop HPC mortar used in this study is a class R4 repair mortar, which is compliant with EN 1504-3 [25] and EN 1504-6 [26] standards. It consists of a brass-covered steel fibre-reinforced mortar specially designed to repair damaged concrete pavements and structures without the need for reinforcing steel

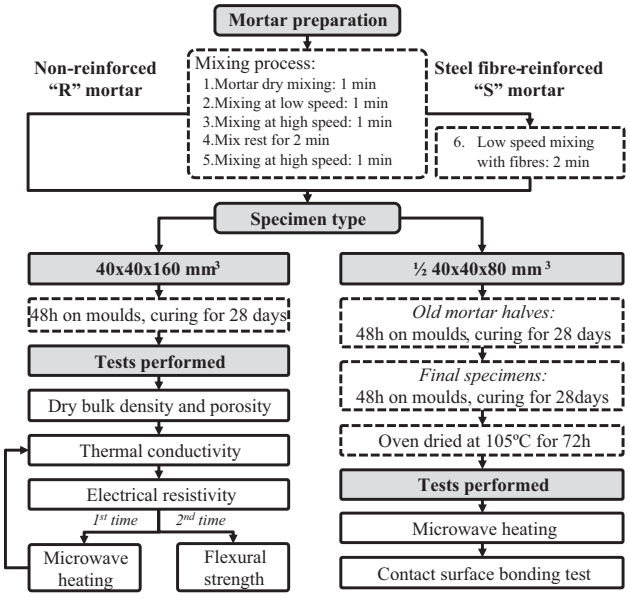

Fig. 1. Experimental programme followed in this study.

bars. According to the specifications of the product, flexural, compressive and adherence strengths were 32 MPa, 130 MPa and higher than 2 MPa, respectively.

Fig. 2 shows the DRAMIX® OL 13/.20 fibres used in this study as a mortar reinforcement. The fibres used were 13 mm long, 0.21 mm in diameter, straight-in-shape brass-covered steel needles. Tensile strength and elastic modulus of the fibres were 2750 MPa and 200000 MPa, respectively. Originally, the mortar was designed to be reinforced with such fibres. However, in order to study the effect of the fibre reinforcement on the mortars exposed to microwave energy, two different mix proportions were used. R reference mortars had the water to mortar total dry weight proportion of 0.12 proposed by the manufacturer. Brass-covered steel fibre-reinforced mortar S was the same mortar but reinforced with steel fibres in a fibre to dry mortar weight ratio of 0.065.

2.2. Specimen preparation

In this study, two different types of specimens were used: $40 \times 40 \times 160\ mm^3$ prismatic specimens prepared in compliance with EN 1015-10 [27] and $40 \times 40 \times 80\ mm^3$ half prismatic specimens.

The mortar mixing process was similar for both specimens. First, dry mortar was mixed for one minute at low speed. Then, water was added and mixed for another minute at the same speed. Immediately after, mortar was mixed for one minute at high speed and then the mixing process was interrupted for two minutes. To finish with the reference mortar mixing process, the mixture was again mixed at high speed for another minute. For the steel fibre-reinforced mortar, an additional step was required. Steel fibres were gradually added to the already mixed R mortar with the mixer working at low speed for another two minutes. As all the mortars used were self-compacting, the mix was poured to the centre of each gap in order to ensure a more symmetric fibre distribution inside the specimens.

For 24 h after making the mix, specimens were cured under ambient laboratory conditions, until the moulds were removed. From that moment, until 28 days curing age was reached, test specimens were submerged in water at 20 °C.

Fig. 3 shows the casting sequence followed for the making of the $40 \times 40 \times 80\ mm^3$ prismatic specimens. As is later discussed, three different bonded surface to load direction angles, β, were studied with the $40 \times 40 \times 80\ mm^3$ specimens. Therefore, the additional metallic pieces placed inside the original moulds were different in each case Fig. 3(a). No matter the case, the manufacturing process of the $40 \times 40 \times 80\ mm^3$ specimens required the casting process previously described to be repeated twice. First of all, non-reinforced old mortar halves were created, see Fig. 3(b). For 24 h after making the mix, the halves were cured under ambient laboratory conditions, until the moulds were removed. From that moment, until 28 days curing age was reached, specimens were submerged in water at 20 °C. Then, half of the halves created were placed in the moulds as indicated in Fig. 3(c) and the remaining gaps were filled with the new mortar (R or S mortar, depending on the case), see Fig. 3(d). Demoulding and the curing procedure was again repeated to complete the specimens required for the bond test. As a consequence, the old half curing time was 56 days while that of the bonded surface and new mortar, was only 28 days.

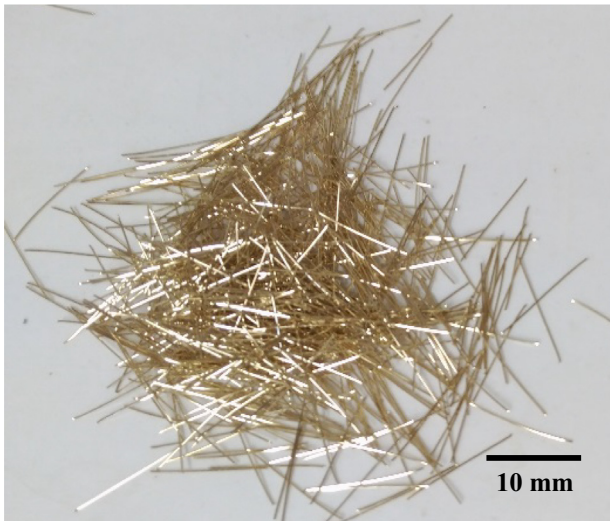

Fig. 2. Brass-covered steel fibres used in this study.

Six specimens were cast for each heating time and mortar type combination, for a total of 48 $40 \times 40 \times 160\ mm^3$ specimens. For the $40 \times 40 \times 80\ mm^3$ specimens, the total number was 144 as each combination involved different heating times, mortar types and load to bonded surface incident angles.

With respect to the tests performed, see Fig. 1, density and porosity were determined just to control the differences between subsequent batches on each mortar. Electrical resistivity and thermal conductivity were measured before and after the microwave heating process with the aim of detecting any minor damage caused by the heating process. At the same time, mechanical damage was also measured via flexural strength and old mortar to new mortar bond tests.

2.3. Dry bulk density and porosity

In order to evaluate the effect of the metallic fibres on the physical properties of the cement mortars after 28 days, dry bulk density (ρ) and water accessible porosity (n) were determined for each $40 \times 40 \times 160\ mm^3$ specimen according to the standard EN 1015-10 [27] with Eqs. (1) and (2):

$$\rho = \rho_w \cdot m_{dry}/(m_{sat} - m_{sub}) \tag{1}$$

$$n = (m_{sat} - m_{dry})/(m_{sat} - m_{sub}) \tag{2}$$

where m_{sat} is the water-saturated mass of the specimens; m_{sub} is the water-submerged mass of the specimens; m_{dry} is the oven-dried mass of the specimens and ρ_w is the water density at testing temperature, as defined by the standard. As the test is done only before the microwave treatment, all the specimens for each cement mortar mixture could be considered equal. As a result, the representative densities and porosities were determined as the average value of all the specimens for each mortar mixture used.

2.4. Thermal conductivity

As a non-destructive test, the thermal conductivity of the hardened mortar (λ) was measured with the aim of determining the damage caused by the microwave energy. Therefore, the thermal conductivity of the hardened mortar was determined for each specimen before, and after, microwave heating treatment based on the Transient Plane Source method developed by Gustafsson [28]. This method has been successfully used to determine thermal properties of highly porous building materials, insulation building materials, hydrating cement pastes and even mortars [29–31].

Fig. 4 shows the setting of the tests carried out with a *HotDisk M1* thermal conductivity tester. Two $40 \times 40 \times 160\ mm^3$ prismatic specimens were used in each test to make a sandwich surrounding the *Kapton 8563 sensor*. The test consists of heating a 19.8 mm diameter disk at a constant P_0 heating rate and measuring the

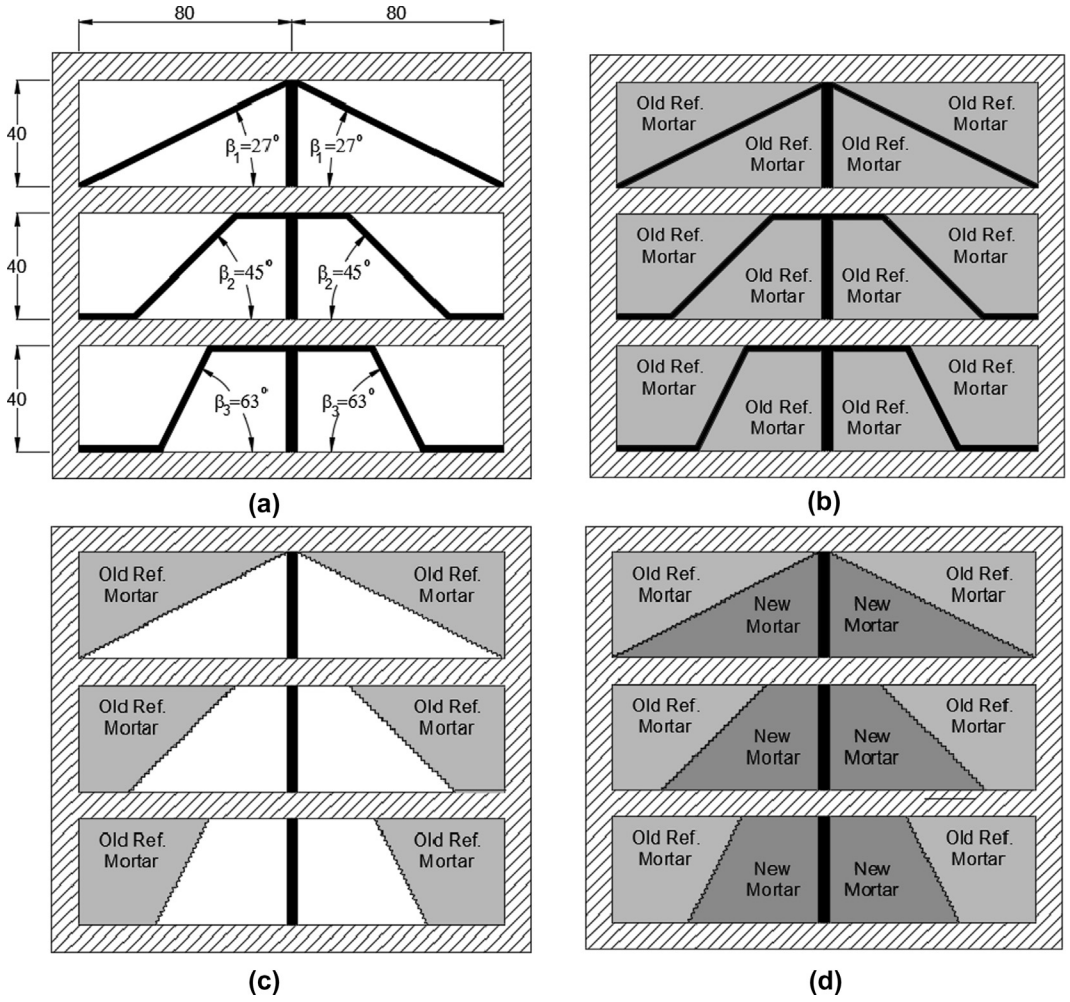

Fig. 3. Making process of the bonded specimens: (a) mould prepared for the making of the first halves; (b) reference old mortar halves casted prior to be demoulded; (c) reference old mortar disposition on the moulds to be bonded to the new mortar halves; and (d) final specimens before being removed. (Figure dimensions in mm).

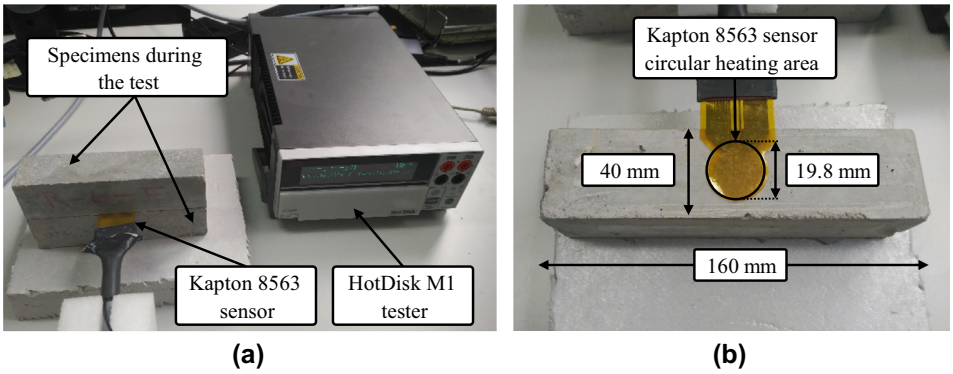

Fig. 4. (a) Set-up for the thermal conductivity test; and (b) Kapton 8563 sensor used.

temperature increment of the disk itself for an initially undetermined time. According to Gustafsson [28], the time-dependent $\Delta T(\tau)$ sensor temperature increase is given by Eq. (3):

$$\Delta T(\tau) = \left(P_0/\left(\pi^{3/2} \cdot a \cdot \lambda\right)\right) \cdot D(\tau) \quad (3)$$

where a is the disk radius, λ is the thermal conductivity of the measured material and $D(\tau)$ is a time dependent dimensionless function that depends on the sensor resistance properties and geometry, as well as on the τ dimensionless time (4):

$$\tau = \sqrt{t \cdot \alpha / a^2} \quad (4)$$

where t is the elapsed time since the beginning of the test, and α is the thermal diffusivity of the material. In this way, the average temperature increment after a relatively short time period only depends on P_0, λ, α and t. According to the TPS theory, the temperature increase is linearly dependent on the $D(\tau)$ function [28]. Therefore, α and λ are obtained via an iterative process by forcing

Eq. (3) to be a straight line. Heating power and testing time were set to 1 W and 20 s respectively, based on preliminary tests.

Initial thermal conductivity of the hardened mortar was determined at an age of 28 days. As the tests are performed on the specimens used to determine both density and porosity of the material, specimens were kept sealed at 25 °C in the laboratory for 2 days in order to cool down and thus ensure their thermal equilibrium. After the microwave heating process, specimens were again kept at 25 °C in the laboratory for another 2 days to recover thermal equilibrium before measuring their thermal conductivity. Thermal conductivity before and after the microwave heating process was calculated as the mean of the 3 tests carried out on each of the 3 pairs of specimens tested, and the mean was also calculated to determine the representative thermal conductivity.

2.5. Electrical resistivity

Electrical resistivity of the hardened mortar was measured with the same goal as for the thermal conductivity: to detect and quantify the damage caused by the microwave energy. For that purpose, an End-to-End AC two-point method was chosen as proposed by Newlands et al. [32]. However, in this case the samples studied were oven-dried before the realisation of the tests.

Fig. 5 shows a scheme of the test. In the test, an *LCR 22821A ohmmeter* was used, connected to two 40×40 mm^2 copper plate electrodes, which were placed on each 40×40 mm^2 specimen face. In order to improve and guarantee an equal specimen to electrode contact on all the samples, a small compressive pressure of 0.6 Mpa was applied with a universal testing equipment. Four different frequencies were initially measured: 100 Hz, 120 Hz, 1000 Hz and 10000 Hz. However, stable results were only obtained for 1000 Hz and 10000 Hz frequencies. Electrical resistivity was obtained according to the second Ohm's law (5):

$$\rho' = r \cdot s/L \tag{5}$$

where r (in Ω) is the electrical resistance of each test specimen; s (in m^2) is the electrode contact area (0.04×0.04 m^2), which is the same as the cross-section of the prismatic sample; and L (in m) is the length of the prism (0.16 m). Finally, the electrical resistivity representative of each tested specimen was determined as the average value of 3 repetitions. For each mortar type and heating time combination, the final representative value was obtained as the mean of the 6 specimens tested.

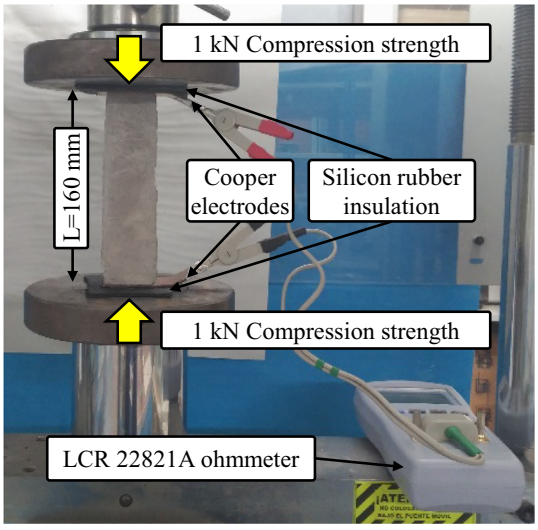

Fig. 5. Disposition of the specimen during the electrical resistivity test.

2.6. Microwave heating

As indicated by Ong and Akbarnezhad [3], microwave heating penetration depth depends mainly on the material dielectric properties and on the heating frequency used. The higher the frequency, the more superficial and local is the heating effect. However, in this case internal disaggregation is desired to remove the highest material amount possible. At the same time, it is also possible to have fibre-reinforced elements attached to other non-reinforced mixes (self-levelling mortars on floor slabs, masonry mortars on building envelopes and so on) that could be replaced by promoting their debonding on the contact surface. For that purpose, the 2.5 GHz frequency available on most of the commercial microwave heaters ensures a proper uniform heating of the concrete specimens [21,33]. At the same time, temperature rise of the heated material is directly proportional to the power used, to the specimen volume and to the heating time. In this case, the heating power was 700 W and three heating times (120 s, 240 s and 600 s) were used and compared to the non-heated samples (0 s). During the heating tests each specimen was surrounded by rockwool insulation, and the specimens were at the same time inside silicone moulds to protect the microwave heater from possible explosions.

2.7. Flexural strength

For the evaluation of the mechanical damage caused by the microwave heating, flexural strength was determined according to the standard EN 1015-11 [34]. In contrast to the tests explained before, this one is destructive; hence it was impossible to determine their value before and after the microwave treatment on the same specimen. Therefore, 6 specimens were tested for each microwave heating time: 0 s, 120 s, 240 s and 600 s for a total of 72 specimens tested. Finally, flexural strength was determined as the mean of the 6 specimens tested.

2.8. Contact surface bonding test

To conclude with the mechanical damage quantification, a new test was defined in this study to determine the influence of the microwave heating on the old mortar to new mortar contact surface bonding conditions under different vertical to horizontal relations, see bonded specimens in Fig. 3. The test consisted of applying a uniform vertical compressive load on the 40×40 mm^2 faces, until specimen failure. A constant load increment of 500 N/s was set, and the maximum displacement was limited to 5 mm for safety reasons. The resulting load-displacement curves presented a sharp load decrease presenting a brittle failure. σ_b, bond load, was determined according to Eq. (6):

$$\sigma_B = F_b/(40 \cdot 40 \cdot \sin\beta) \tag{6}$$

where F_b is the maximum load registered during the test, and β is the existing angle between the load direction and the bond surface, which was 27°, 45° or 63° depending on the case, see Fig. 3(a). For each heating time, mortar type and β angle combination, the final representative result was obtained as the mean value of six specimens tested.

3. Results and discussion

3.1. Microwave heating effect on the thermo-physical properties

Firstly, dry density and porosity obtained for each mortar were analysed in order to control the specimen homogeneity between different batches. Mean dry densities for the R and S mortars were 2.27 kg/m^3 and 2.34 kg/m^3, with a standard deviation of 0.02 kg/m^3

and 0.03 kg/m^3, respectively. As expected, the density of the fibre-reinforced mortar was higher than that of the reference mortar, due to the higher density of the fibres. According to the porosity, S mortar presents higher values than R mortar, with a mean value in percentage by volume of 12.1% and 9.4%, respectively, which was also observed for previous fibre-reinforced mortars studied [35].

In addition, Fig. 6 shows the thermal conductivity of both R and S mortars before and after the microwave heating treatment. As the test is non-destructive, both tests were done on the same specimen. Therefore, results before and after the microwave heating process are directly comparable. For the R mortar, see Fig. 6(a), taking into account all the specimens, the thermal conductivity before MW heating was 1.65 W/mK with a standard deviation of 0.02 W/mK. The heat treatment applied caused a general decrease of the thermal conductivity. The higher the heating time, the greater was this reduction. Thermal conductivity decreased by 1%, 5.3% and 9.3% for 120 s, 240 s and 600 s heating times, respectively. This diminution was mainly caused by the sample's water loss. In spite of being oven-dried to reach constant mass for at least 72 h, specimens lost more water due the higher and more intense heating power applied by the microwaves. This was evident as the microwave walls were wet after each heating process. In an oven, temperature gain comes from the heat exchanging process on the specimen surface. Therefore, the temperature of the specimen is always higher on the surface than on the inside, creating a temperature and moisture gradient that eases the water evacuation without creating high inner pressures. On the contrary, 2.5 GHz microwaves induce a nearly uniform internal heat generation, which is enhanced by the water presence. In this case, heat is released from the specimen to the microwave heating chamber, hence the temperature on the inner part would be higher than that of the surface, creating a faster moisture migration from the inner pores to the specimen surface. As the pore pressure is higher for the MW heating process, part of the remaining water finds a way to leave the material, reducing its water content and decreasing the thermal conductivity of the bulk material. When the pore pressure exceeds the mortar tensile strength, pore pressure is released by spalling the mortar from the inside [4]. This effect was observed on the R mortar specimens initially planned to be heated for 600 s. After an elapsed time of 300–400 s, all the specimens spalled, as is later discussed in Section 3.2. Nonetheless, thermal conductivity measured for the remaining fragments indicated that the non-broken parts had similar values to that expected in a non-damaged material.

For the S mortar, see Fig. 6(b), a dissimilar behaviour was observed. Taking into consideration all the specimens, the thermal conductivity before MW heating was 1.88 W/mK with a standard deviation of 0.14 W/mK. In any case, thermal conductivity of the S mortar was significantly higher than that of the R mortar, which is attributed to the high steel fibre density of the mix and to the higher thermal conductivity of the steel fibres with respect to the rest of the mortar components, though, the standard deviation indicates that the initial thermal conductivity is much more dispersed for the S mortar, which is thought to be caused by the randomness of the fibre distribution in the specimens. With respect to the MW heating effect, the heat treatment applied caused a decrease of 7.1% and 6.2% for the 120 s and 600 s heating times, respectively. However, a thermal conductivity increase of 2.8% was detected for the 240 s heating time, which is within the 5% error attributed to the accuracy of the test itself.

During the MW heating, moisture migration occurs in the specimen from the inside to its surface due to the generated temperature gradient. For low heating times, water near the specimen surface finds a way out and therefore caused a thermal conductivity decrease. However, as the heating continues, water from the inside is transported to more superficial pores, but has no time to reach the surface, increasing thermal conductivity on the surface. Finally, for the highest heating time, the water on the surface is removed and the thermal conductivity is decreased again.

Unlike the R mortar, S mortar did not break for any of the heating times applied. The higher porosity of the mortar contributed to diminishing the internal pore pressure increase caused by the temperature gradient. At the same time, the flexural strength reduction observed indicated that the MW treatment damaged the specimen paste, enhancing the water migration and thus reducing the pore pressure. Furthermore, the reinforcing action of the steel fibres also contributed to maintain the integrity of the cement mortar.

As the electrical resistivity test is also non-destructive, results before and after the microwave heating process were also directly comparable. Fig. 7 shows the electrical resistivity obtained for R and S mortars. Based on the results, it seems legitimate to affirm that electrical resistivity was reduced with the heating time for the R mortar, see Fig. 7(a). For the highest heating time, measurement was impossible as the specimens spalled after an elapsed time of 300–400 s. Although the decreasing tendency was similar for both frequencies, there is not a clear preferential frequency to use as the differences between the "before" and "after" results are greater for different frequencies depending on the studied

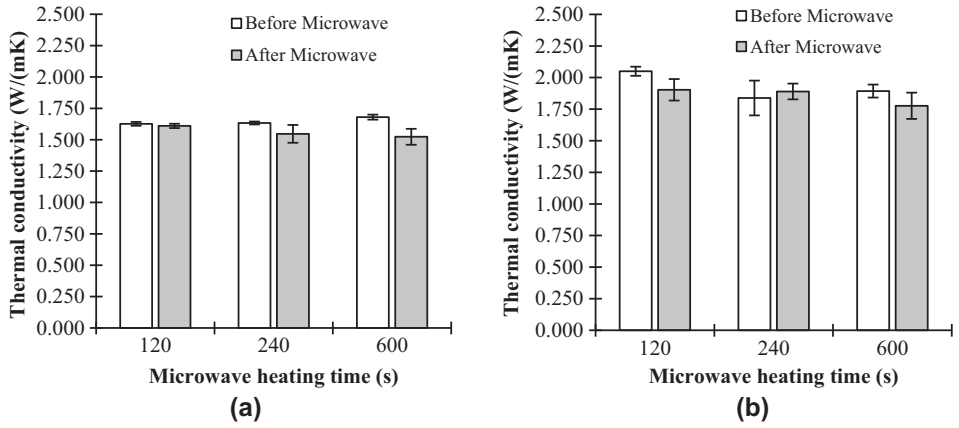

Fig. 6. Influence of the microwave heating time on the mortar thermal conductivity: (a) non-reinforced reference mortars (R-mortars); and (b) steel fibre-reinforced mortars (S-mortars).

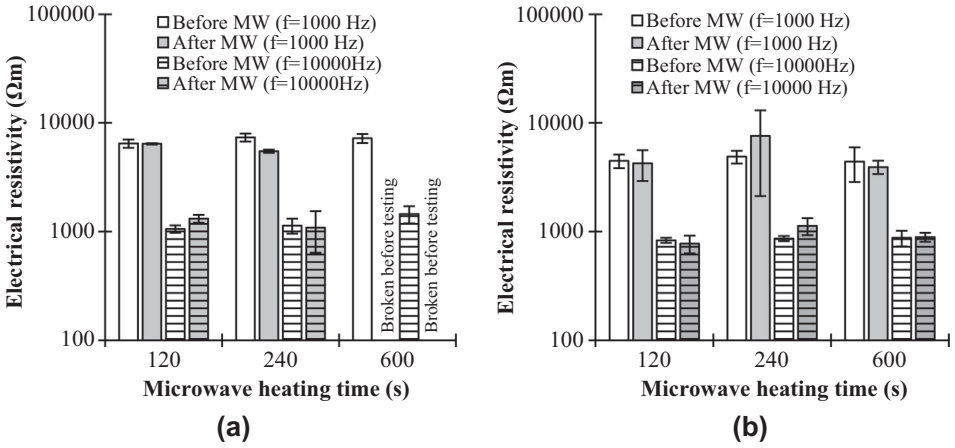

Fig. 7. Influence of the microwave heating time on the mortar electrical resistivity: (a) non-reinforced reference mortar (R-mortars); and (b) steel fibre-reinforced mortar (S-mortars).

heating time. The electrical resistivity decrease for the R mortar is higher for the 120 s heating time and a frequency of 1000 Hz, while the opposite occurred for the 240 s heating time and 10000 Hz frequency. As for the thermal conductivity, electrical resistivity presents a more chaotic behaviour for the S mortar than that of the R mortar, see Fig. 7(b). For 120 s and 600 s MW heating times, electrical resistivity is reduced for both frequencies, but the opposite behaviour is observed for the 240 s heating time. The authors do not find any explanation for this behaviour, as an electrical resistance increase was expected due to the capillary water content reduction suffered by both mortars [32]. Therefore, the authors concluded that electrical resistivity is not an effective parameter to detect damages on steel fibre-reinforced mortars in the way it was measured in this study.

3.2. Surface temperature on the specimens heated by microwaves

A further test was performed to estimate the surface temperature of the specimens as a function of the MW heating time. For that purpose, a *"Testo 875i"* infrared thermographic camera was used. The camera works on a temperature range from 0 to 350 °C with an accuracy of 2 °C. In order to calibrate the camera for the studied mortar, three calibration specimens were heated to 105 °C for 24 h (one for each mortar studied). Based on the temperature recorded for a black body at the same temperature, emissivity of the R and S mortars was determined to be 0.93.

Fig. 8 shows the temperature of both R and S mortars for 120 s, 240 s and 300 s MW heating times. According to the results, R mortar reached a maximum temperature of 108 °C, 182.9 °C and 250.9 °C for 120 s, 240 s and 300–400 s MW heating times, respectively. Therefore, the temperature rise was almost linear during all the process up to the spalling time. In the same cases, the maximum temperatures for the S mortar were significantly higher, 215.8 °C, 276.1 °C and 348.7 °C (based on the temperature range of the camera, the last value could be even higher than that measured). This increase indicated that the steel fibre presence clearly enhanced the heating effect on the specimen surface due to microwave energy. It is well known that steel tends to reflect most of the microwave energy, which enhances the heating effect near the reinforcement [3]. This effect would be beneficial when superficial damage is desired, for example to remove the damaged concrete cover layer. However, the high fibre density used in this study concentrated the temperature rise on the specimen surface. Despite the high surface temperature, S mortar resisted surface delamination due to the fibre reinforcing capacity.

Fig. 9 shows a schematic representation of the most plausible fracture process for the spalled R mortar. Temperature distribution observed for the R mortar after microwave heating for 240 s indicated a higher heating close to the ends of the specimens, which is attributed to the higher exposition to radiation due to its contour effect [3]. As the specimens were oven-dried before the microwave heating process, specimen pores near the surface were non-saturated. However, in a more interior hot spot near the specimen end surface, pores were still partially or fully water saturated, leading to the fracture initiation. Then, fracture propagation occurred in apparently random directions, but showing two preferential planes: one was the 40×40 mm^2 cross-section, and the other, an intermediate 40×160 mm^2 cross-section.

3.3. Microwave heating influence on the mechanical properties

Microwave influence on the mechanical properties was determined by flexural strength tests. Fig. 10 shows the flexural strength of the R and S mortars as a function of the MW heating time applied. For the R mortar, flexural strength decreased gradually from 14.9 MPa to 7.5 MPa up to 240 s MW heating time, which indicates an evident deterioration of the mechanical properties. Then, spalling occurred after an elapsed time of 300–400 s, reducing the specimen to small fractions as can be seen in Fig. 9. The fibre presence on the S mortar changed this behaviour dramatically. The initial value of 31.3 MPa is in accordance with the strength reported by the manufacturer, which is at the same time significantly higher than that of the reference mortar. Therefore, steel fibre presence increased effectively both the initial flexural strength and residual strength. Due to the MW heating process, flexural strength was reduced by 13% on average. Nevertheless, for the S mortar the reduction was similar and independent of the MW heating time applied, which indicates that the damage mainly occurred during the initial part of the heating process. For the first 120 s, flexural strength reduction ratio was 0.04 kN/s and 0.0375 kN/s for the R and S mortars, respectively. As this reduction was similar for both mortars, Authors concluded that MW heating damaged the cement mortar matrix almost equally during the 0–120 time interval. However, this initial damage was sufficient to connect the non-connected pores, easing the remaining water evacuation. This stage may occur slightly before the above mentioned 120 s, or slightly after them. This is the reason that may lead to higher standard deviations of the flexural strength values shown in Fig. 10. Although mitigated, pore pressure rise continued, causing the progressive damage observed on the R

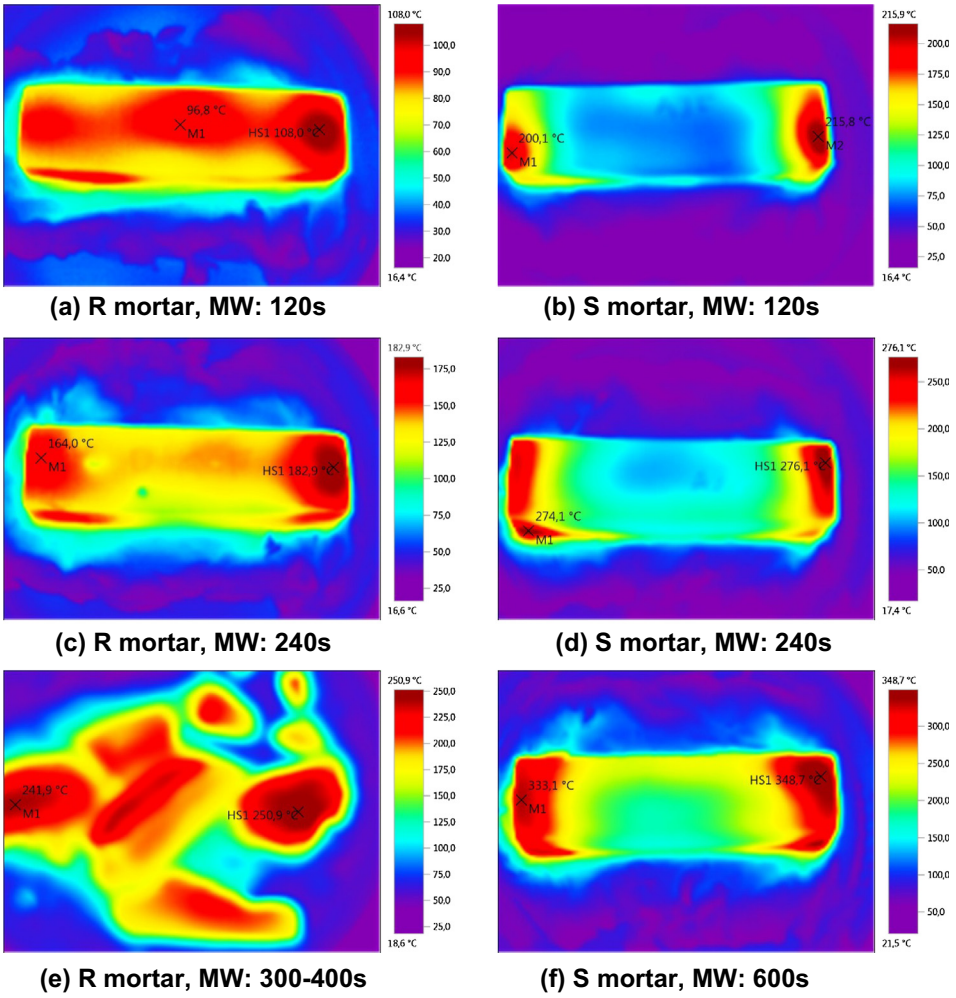

Fig. 8. Temperature distribution just after the MW heating time for R and S mortars.

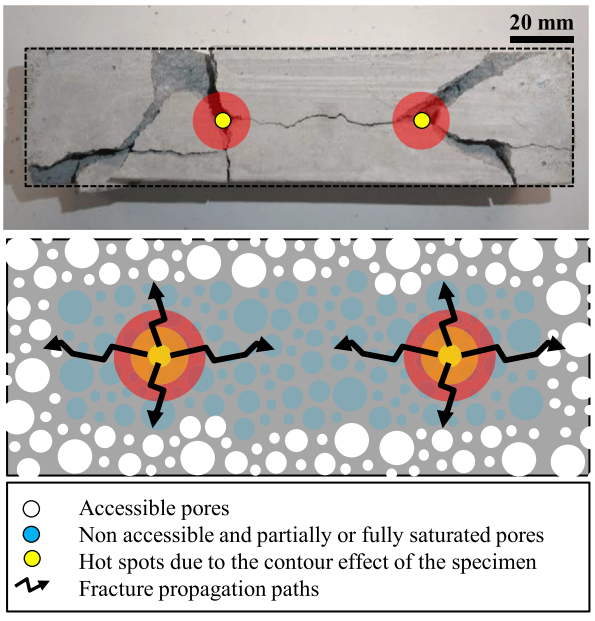

Fig. 9. Reconstruction of a spalled reference mortar specimen after microwave heating for 300–400 s and fracture initiation and propagation on the prismatic specimens.

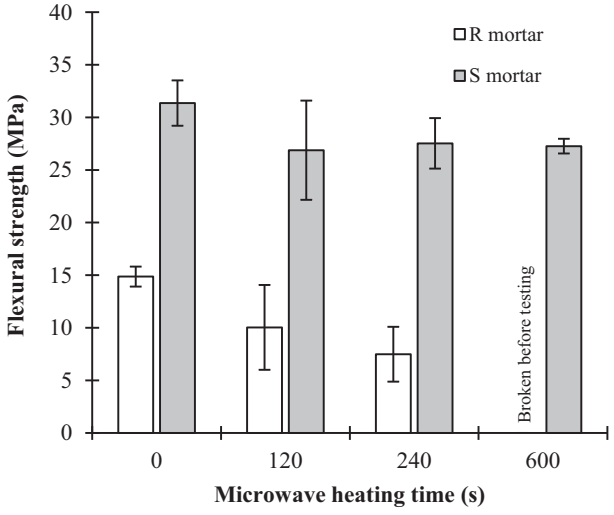

Fig. 10. Flexural strength of the reference (R mortar) and steel fibre-reinforced (S mortar) mortars before, and after, the microwave heating process.

mortar. However, the fibre-reinforcement of the S mortar focused the heat rise mainly on the specimen surface, while the fibres began to act resisting the pressure increase associated with the temperature rise, preventing any damage increment from then on.

Based on the flexural strength results, it could be concluded that the MW heating would be an option when the mortars were not reinforced with steel fibres but for the S mortar, MW damage would be insignificant. With the aim of studying the influence of the MW heating effect on the steel fibre to mortar bond strength, mortar U_{rel} relative toughness was determined on the flexural specimens from the F_{max} maximum load to n load reductions of 25%, 50% and 75% according to Eq. (7):

$$U_{rel} = (1/F_{max}) \cdot \int_{x(F_{max})}^{x(n \cdot F_{max})} F(x) \cdot dx \quad (7)$$

where x is the specimen deflection recorded during the flexural test.

Fig. 11 shows the relative toughness results for the S mortar, as well as its reduction with respect to the unheated mortar specimens. As the MW heating time increased, a more severe reduction of the specimen toughness was observed, see Fig. 11(a). This effect was evident as the relative toughness reduction curves tended to have a constantly increasing value, see Fig. 11(b). From the comparison between the curves representing the different maximum strength reductions, it was also concluded that most of the residual stress reduction occurred just after the crack initiation. At the beginning, most of the fibre-reinforcement comes from the fibre to cement paste bond strength. Once the crack begins to propagate, fibre residual stress is more attributed to the curvature of the fibres, therefore the residual strength mainly is caused by the friction of the fibre with the cement paste.

Based on the flexural strength, it would seem legitimate to affirm that R mortars were susceptible to MW heating but steel fibre-reinforced S mortars were not. Nevertheless, the microwave reflecting effect observed on the S mortar specimen surface could be interesting when steel fibre-reinforced mortars are bonded to a non-reinforced concrete or mortar, such as the R mortar. Microwave energy would be projected back to the R mortar from their bonding surface. Due to microwave reflection, non-reinforced concrete would suffer a higher temperature rise near the bond surface, promoting its debonding or internal spalling.

Fig. 12 shows the bond load obtained as a function of the mortar type, MW heating time and bond surface to compressive load direction angle. Note that the σ_b bond load is the result of dividing the compressive load applied by the bond surface, not the specimen cross section. However, total stress results are only discussed as a further analysis of the normal and tangential stresses led to no more meaningful information.

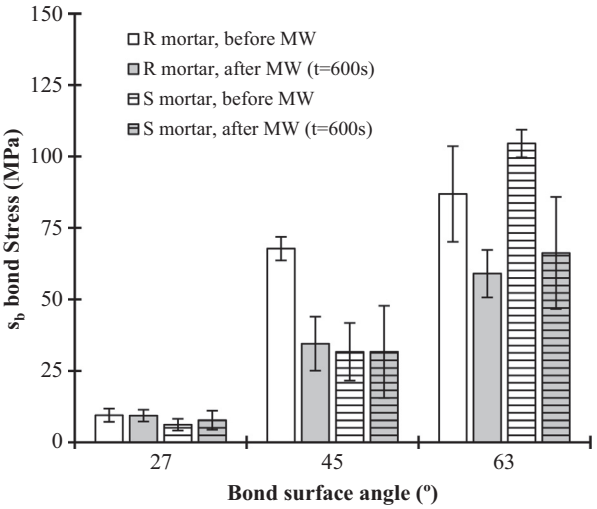

Fig. 12. Influence of the bond to surface angle on the mortar's bond strength.

Before the MW heating process, R mortar bond strength was negligibly higher than that of the S mortar; for the intermediate angle, the R mortar nearly doubled its value, while for the highest angle, the bonding strength was higher for the S mortar. After the MW heating process, a dissimilar influence was observed depending on the bond surface angle studied. For the lowest angle, no significant influence was observed due to the MW heating process. For the intermediate angle, a clear influence was observed for the R mortar, but a negligible effect on the S mortar. Finally, a similar reduction was detected on the highest angle for both mortars.

The results obtained for the 27° and 45° bond surface angles indicated that the bond strength in general was better when old R mortar was bonded to new R mortar, meaning that the fibre presence had a negative effect on the bonding process. On the contrary, 63° bond surface results showed that damage existed due to the MW heating process. As shown in Fig. 13, specimens with 27° and 45° bond surfaces failed due to debonding of the generated interface. However, for the 63° case, the failure occurred on the half corresponding to the R mortar, denoting that the damage mainly occurs on the R mortar bulk material. This could also be seen on the failure sequence of each specimen tested, especially on the S mortar.

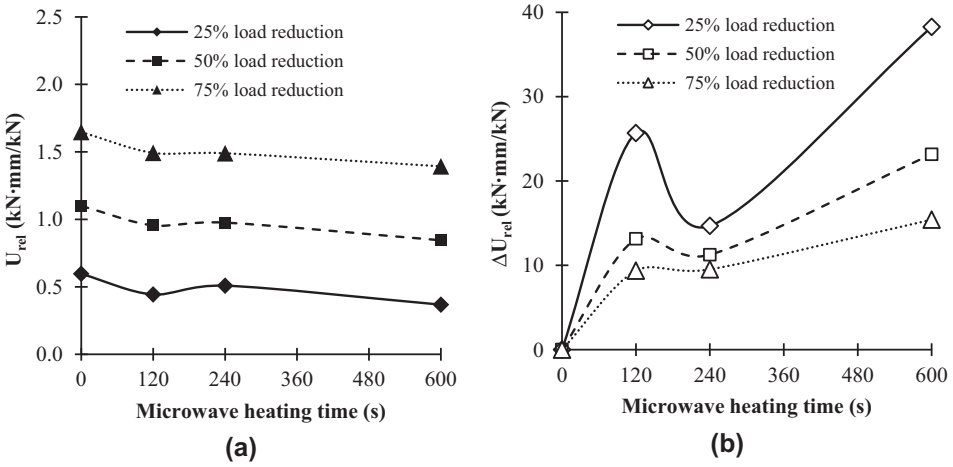

Fig. 11. (a) Relative toughness, and (b) relative toughness reduction due to the MW heating process for the steel fibre-reinforced mortars (S mortars).

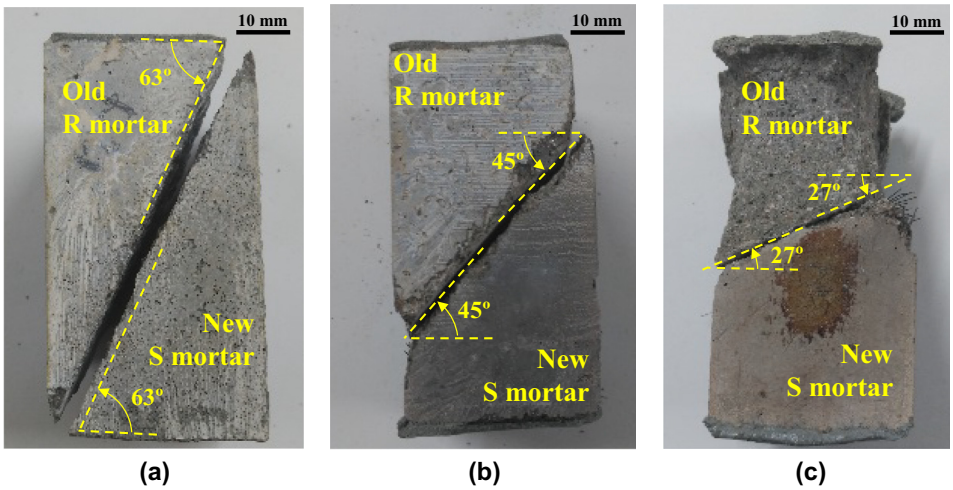

Fig. 13. Prevailing failure modes observed for each bond surface angle for the steel fibre-reinforced mortars: (a) $\beta = 63°$; (b) $\beta = 45°$; (c) $\beta = 27°$.

4. Conclusions

This paper analysed the influence of using microwave heating as a demolition/debonding thermal process on steel fibre-reinforced mortars used to repair structures. In particular, it analyses the influence of the steel fibre presence on its thermal and mechanical behaviour. For that purpose, the same mortars with, and without, steel fibres have been tested before, and after, applying the microwave heating process by both destructive, and non-destructive, tests. Based on the results, the following conclusions have been obtained:

- The thermal conductivity of the steel fibre-reinforced mortar was on average 14% higher than that of the non-reinforced reference mortar. Furthermore, thermal conductivity of both mortars decreased by up to 7% due to the thermal process, which is attributed to the water loss caused by the microwave based internal heat generation. Nevertheless, the absence of any damage to thermal conductivity correlation does not encourage the use of this property to monitor the mortar damage.
- Electrical resistivity is not an effective parameter to detect damages caused by microwave heating on steel fibre-reinforced mortars the way it was measured in this study.
- Flexural strength is reduced by 32% and 50% for 120 s and 240 s microwave heating times for the reference mortar, while total failure occurred for an elapsed time of 300–400 s. The water found on the microwave walls indicated that, despite the oven-drying process, specimens still had water in non-accessible pores, being the main reason for spalling to occur.
- Mortar surface temperature is increased by 200%, 150% and 140% with the steel fibre presence for the 120 s, 240 s and 300 s heating times used in this study. However, flexural tests indicated that the damage caused by the microwave heating process is negligible on the steel fibre-reinforced mortars. Porosity increase caused in the mortar contributed to maintaining the integrity of the mortar by mitigating the internal pore pressure increase caused by the heating process.
- In spite of the slight damage caused by the microwave heating process on the steel fibre-reinforced mortars, the reduction of up to 40% of the relative toughness obtained indicated that the microwave heating damage has more influence on the mortar behaviour just after the crack initiation.
- According to the bond strength, based on the failure modes observed on the specimens, the microwave heating process mainly influenced the results by weakening the weakest mortar resistance, but no significant influence was detected on the bond strength itself.

Finally, this paper shows the results obtained for the first research phase focused on evaluating the viability of the microwave demolition method on steel fibre-reinforced cement composites. The method proposed studied the damage by using only one type of specimen and fibre proportion, which might influence the fibre spatial distribution. Influence of the heating frequency is also limited to 2.5 GHz. All this influences will be further studied.

Conflict of interest

None.

Acknowledgements

This work has been partly financed within the European Horizon 2020 Joint Technology Initiative Shift2Rail through contract no.730841. The authors also wish to thank the Basque Government for financial assistance through IT919-16 and through the project Elkartek 2018: GOLIAT: "Aplicaciones electromagnéticas para usos y entornos industriales severos" (Electromagnetic applications on severe industrial environments). Finally, the authors are also grateful to MAPEI for the donation of the mortars used in this study.

References

[1] P. Lindsell, Demolition techniques for concrete structures, in: P.C. Kreijger (Ed.), Adhesion Problems in the Recycling of Concrete, Springer, US, Boston, MA, 1981, pp. 201–215.
[2] Y. Kasai, Demolition of concrete structure by heating, Concr. Int. 11 (1989) 33–38.
[3] K. Ong, A. Akbarnezhad, Microwave-Assisted. 6000 BROKEN SOUND PARKWAY NW, STE 300, BOCA RATON, FL 33487–2742, Concrete Technology: Production, Demolition and Recycling, 1st ed., CRC Press TAYLOR & FRANCIS GROUP, USA, 2015.
[4] N. Makul, P. Rattanadecho, D.K. Agrawal, Applications of microwave energy in cement and concrete - a review, Renew. Sustain. Energy Rev. 37 (2014) 715–733.
[5] M.Q. Feng, F. De Flaviis, Y.J. Kim, Use of microwaves for damage detection of fiber reinforced polymer-wrapped concrete structures, J. Eng. Mech. 128 (2002) 172–183.
[6] Y.J. Kim, L. Jofre, F. De Flaviis, M.Q. Feng, Microwave reflection tomographic array for damage detection of civil structures, IEEE Trans. Antennas Propag. 51 (2003) 3022–3032.
[7] Y.J. Kim, L. Jofre, F. De Flaviis, M.Q. Feng, Microwave subsurface imaging technology for damage detection, J. Eng. Mech. 130 (2004) 858–866.
[8] J. Nadakuduti, G. Chen, R. Zoughi, Semiempirical electromagnetic modeling of crack detection and sizing in cement-based materials using near-field microwave methods, IEEE Trans. Instrum. Meas. 55 (2006) 588–597.
[9] T. Yu, Distant damage-assessment method for multilayer composite systems using electromagnetic waves, J. Eng. Mech. 137 (2011) 547–560.

[10] G. Roqueta, L. Jofre, M.Q. Feng, Analysis of the electromagnetic signature of reinforced concrete structures for nondestructive evaluation of corrosion damage, IEEE Trans. Instrum. Meas. 61 (2012) 1090–1098.
[11] Wu. Xuequan, Dong Jianbgo, Tang Mingshu, Microwave curing technique in concrete manufacture, Cem. Concr. Res. 17 (1987) 205–210.
[12] R.G. Hutchison, J.T. Chang, H.M. Jennings, M.E. Brodwin, Thermal acceleration of Portland cement mortars with microwave energy, Cem. Concr. Res. 21 (1991) 795–799.
[13] C.K.Y. Leung, T. Pheeraphan, Microwave curing of Portland cement concrete: experimental results and feasibility for practical applications, Constr. Build. Mater. 9 (1995) 67–73.
[14] C.K.Y. Leung, T. Pheeraphan, Very high early strength of microwave cured concrete, Cem. Concr. Res. 25 (1995) 136–146.
[15] M. Oriol, J. Pera, Pozzolanic activity of metakaolin under microwave treatment, Cem. Concr. Res. 25 (1995) 265–270.
[16] D. Sohn, D.L. Johnson, Microwave curing effects on the 28-day strength of cementitious materials, Cem. Concr. Res. 29 (1999) 241–247.
[17] A. Korpa, R. Trettin, Very high early strength of ultra-high performance concrete containing nanoscale pozzolans using the microwave heat curing method, Adv. Cem. Res. 20 (2008) 175–184.
[18] P. Rattanadecho, N. Suwannapum, B. Chatveera, D. Atong, N. Makul, Development of compressive strength of cement paste under accelerated curing by using a continuous microwave thermal processor, Mater. Sci. Eng. A 472 (2008) 299–307.
[19] N. Makul, B. Chatveera, P. Ratanadecho, Use of microwave energy for accelerated curing of concrete: a review, Songklanakarin J. Sci. Technol. 31 (2009) 1–13.
[20] E. Jerby, O. Aktushev, V. Dikhtyar, Theoretical analysis of the microwave-drill near-field localized heating effect, J. Appl. Phys. 97 (2005).
[21] A. Akbarnezhad, K.C.G. Ong, M.H. Zhang, C.T. Tam, T.W.J. Foo, Microwave-assisted beneficiation of recycled concrete aggregates, Constr. Build. Mater. 25 (2011) 3469–3479.
[22] M. Tsujino, T. Noguchi, R. Kitagaki, H. Nagai, Ompletely recyclable concrete of aggregate-recovery type by using microwave heating, J. Struct. Constr. Eng. 76 (2011) 223–229.
[23] Y. Menard, K. Bru, S. Touze, A. Lemoign, J.E. Poirier, G. Ruffie, et al., Innovative process routes for a high-quality concrete recycling, Waste Manage. 33 (2013) 1561–1565.
[24] A. Bentur, S. Mindess, Fibre Reinforced Cementitious Composites, CRC Press, 2006.
[25] EN 1504-3. Products and systems for the protection and repair of concrete structures. Definitions, requirements, quality control and evaluation of conformity. Part 3: Strectural and non-structural repair (2006).
[26] EN 1504-6. Products and systems for the protection and repair of concrete structures. Definitions, requirements, quality control and evaluation of conformity. Part 6: Anchoring of reinforcing steel bar (2007).
[27] UNE-EN 1015-10. Methods of Test for Mortar Masonry. Part 10: Determination of Dry Bulk Density of Hardened Mortar (2007).
[28] S.E. Gustafsson, Transient plane source techniques for thermal conductivity and thermal diffusivity measurements of solid materials, Rev. Sci. Instrum. 62 (1991) 797–804.
[29] A. Bouguerra, A. Aït-Mokhtar, O. Amiri, M.B. Diop, Measurement of thermal conductivity, thermal diffusivity and heat capacity of highly porous building materials using transient plane source technique, Int. Commun. Heat Mass Transfer 28 (2001) 1065–1078.
[30] S.A. Al-Ajlan, Measurements of thermal properties of insulation materials by using transient plane source technique, Appl. Therm. Eng. 26 (2006) 2184–2191.
[31] D.P. Bentz, Transient plane source measurements of the thermal properties of hydrating cement pastes, Mater. Struct. 40 (2007) 1073–1080.
[32] M.D. Newlands, M.R. Jones, S. Kandasami, T.A. Harrison, Sensitivity of electrode contact solutions and contact pressure in assessing electrical resistivity of concrete, Mater. Struct. 41 (2008) 621–632.
[33] J. Norambuena-Contreras, Gonzalez-Torre I. Influence of the microwave heating time on the self-healing properties of asphalt mixtures, Appl. Sci. 7 (2017).
[34] UNE-EN 1015-11. Methods of Test for Mortar for Masonry. Part 11: Determination of Flexural and Compressive Strength of Hardened Mortar (2007).
[35] J. Norambuena-Contreras, C. Thomas, R. Borinaga-TreviÃño, I. Lombillo, Influence of recycled carbon powder waste addition on the physical and mechanical properties of cement pastes, Mater. Struct. 49 (2016) 5147–5159.